17

Image Post-Processing and Interpretation

Masahiro Jinzaki, Minoru Yamada and Sachio Kuribayashi
Dept. of Diagnostic Radiology, Keio University School of Medicine
Japan

1. Introduction

Image post-processing is defined as the process of integrating a series of axial images into a form that is often easier to interpret than the sections themselves. The source transverse section is a fundamental image for interpretation. However, because of the complexity of coronary anatomy, interpreters must review coronary CT angiography interactively on workstations capable of 3-dimensional (3D) displays. The 3D data set can be reformatted according to the needs of the investigator using several types of post-processing algorithms. Coronary artery interpretation includes assessment of calcium scoring on non-contrast image and coronary angiography on enhanced image. Non-coronary cardiovascular findings and extra-cardiac findings should be reviewed in addition to recognize primary and secondary comorbid pathology and to identify findings that lead to alternative non-cardiovascular diagnoses. The ultimate objective of post-processing and interpretation is to convey diagnostic information to the treating physician with as much clarity and accuracy as possible. Interpretation times vary, usually depending on the image quality and the user's experience and knowledge of cardiac CT and the individual workstation. Normally, experienced users usually spend no more than 10 minutes segmenting and interpreting cardiac CT studies.

2. Post-processing technique

The source transverse sections are the primary tools for interpretation of coronary CT angiography examinations. Post-processing imaging is performed from reconstructed axial images and is useful in allowing clinically relevant information to be extracted from large number of axial images. In addition, the diagnostic accuracy of axial images (86% sensitive and 78% accurate) for the detection of coronary stenosis is low compared with combination of post-processing techniques (98% sensitive and 94% accurate) (Jinzaki et al, 2009). Thus, the review of 3D displays is necessary for the coronary artery interpretation due to the complexity of coronary anatomy. These include volume rendering, multiplanar reformation, thin-slab maximum intensity projection, curved multiplanar reformation, angiographic view, and plaque-loaded angiographic view. A post-processing image which enables the evaluation of coronary artery disease with fewer images and one that is understandable to the third person is preferable.

2.1 Multiplanar reformation (MPR)
MPR is a high-resolution reconstruction format that allows display of planar images at any angular section through the acquisition volume, which permits visualization in not only the

axial plane but also in orthogonal (coronal and sagittal) or oblique planes that better follow the arterial course in the thorax. The slice thickness can be modified, and a thick slab may be helpful in visualizing tortuous coronary artery. MPR is a simple algorithm which can be rendered quickly and accurately on any image-processing workstations. The distance measurements in MPR are accurate. Different structures in MPR are accurate and do not overlap. There is no loss of voxel value information due to threshold.

MPRs are best suited for evaluation of the individual cardiac chambers, aorta (Fig. 1), and pulmonary vasculature with cardiac CT. MPRs are also well suited for selective evaluation of a coronary short segment. If a narrowing is suspected on axial views, display in coronal or sagittal orientations can confirm the presence of a stenosis (Fig. 2).

The disadvantage of MPR is that only short segments can be analyzed at a time due to the nonlinear pathway of the coronary arteries. Thus, MPR requires the creation of numerous images in different planes at every suspected location of coronary stenosis. Furthermore, it is less suited for displaying the length of an artery. Grading of a stenosis is not advisable with coronal, sagittal, or oblique reconstructions alone, because of partial averaging (Johnson et al, 2010).
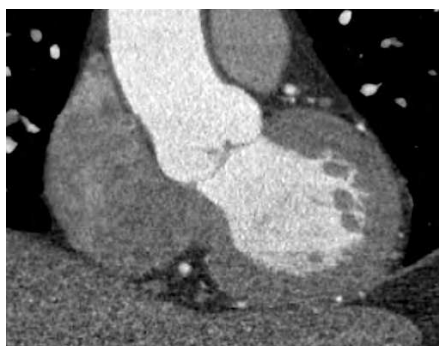

Fig. 1. Multiplanar reformation of cardiac structure

Oblique coronal image orientate better the planes of the geometrical orientations of cardiac structure (left chamber and aorta).

a)   b)   c)
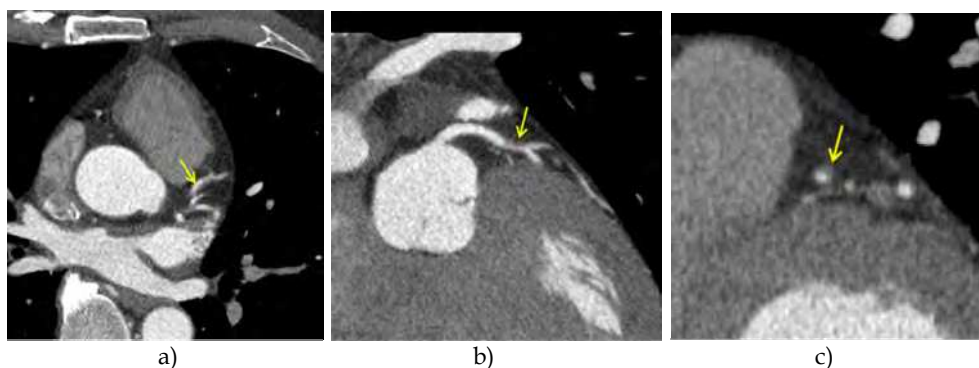
Fig. 2. Multiplanar reconstruction of coronary stenosis

When a narrowing (arrow) is suspected on axial views (a), multiplanar reformation can be used to set the planes (b, c) in an orientation that matches one of the coronary short segments.

2.2 Thin-slab maximum intensity projection (Thin-slab MIP)

In both thin-slab MIP and MPR, orthogonal or oblique planes can be reviewed interactively. MIP is a projection technique, in which only the highest density pixel in the projection direction is displayed to reconstruct the two-dimensional images. MIP image allows the differentiation between enhanced vascular structures and non-vascular structures, because the result is a projection of the highest density. In practice, MIP is usually performed interactively with a sliding slab, enabling the radiologist to adjust the window, select the optimal orientation to display each artery, and modify the slab thickness (Fishman et al, 2006).

The advantage of thin-slab MIP is the creation of a vascular map quickly without modification of several parameters (Fig. 3). In addition, MIP is better for displaying small-caliber segments: the minimum vessel diameter seen with MIP was 0.7 mm versus 1.5 mm for volume rendering (VR) (Zhang et al, 2004). This is because MIP is designed to selectively demonstrate the arterial vasculature, which involves selection of the highest attenuation voxels along rays projected through the volume. It is controversial whether thin-slab MIP can be used for the diagnosis of coronary artery stenosis. One study compared interpretation of 3 sets of orthogonally oriented thin-slab MIPs with axial sections with 16-slice CT (Choi et al, 2006). For all three radiologists, the Az (area under the ROC curve) values from the MIP images were higher than those Az values from the transaxial images, however, the difference was significant for only one reader.

MIP has a tendency to overestimate stenosis. Heavily calcified arteries cannot be evaluated with MIP. Thus, thin-slab MIP cannot be used for the quantity evaluation of plaque, including the determination of grading of a stenosis. In addition, numerous images in different planes are required for the evaluation of the whole coronary arteries. Thin-slab MIP is useful as an adjunct to VR. However, it should not be the sole technique used for interpretation.

a)   b)   c)
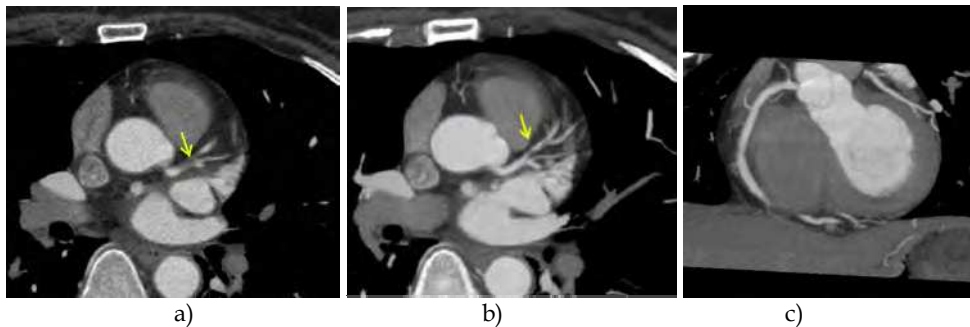
Fig. 3. Thin-slab maximum intensity projection of coronary stenosis

When a narrowing (arrow) is suspected on axial views (a), the use of thin-slab maximum intensity projection (b) increases the overview of each coronary artery. Thin-slab maximum intensity projection enables creation of a vascular map (c) quickly without modification of several parameters.

2.3 Curved multiplanar reformation (curved MPR)

The development of curved MPR format made it possible for the interpreter to follow the course of a tortuous vessel for longer distances as it changes direction (Fig. 4) (Ferencik et al., 2007). The artery can be displayed as a straight line (Fig. 5). This method enables one entire coronary artery to be followed and displayed in one reconstruction, and reduces the number of planar images needed, compared with MPR. An automated program is possible to track the coronary arteries using placement of a single point in any portion of each artery or ascending aorta, the computer can trace a given coronary vessel departing proximally and distally from the point chosen, and extract the images in seconds. Other automated program tracks the path of the coronary artery, when the operator selects two points: one at the beginning and one at the end of the vessel. These applications also provide MPRs that are orthogonal to the vessel centerline, thus creating cross-sectional cuts of each coronary arterial segment (Fig. 5). All other surrounding structures are automatically eliminated that are any distance from this centerpoint, possibly decreasing problems seen with other reconstruction methods from tortuosity and overlap.

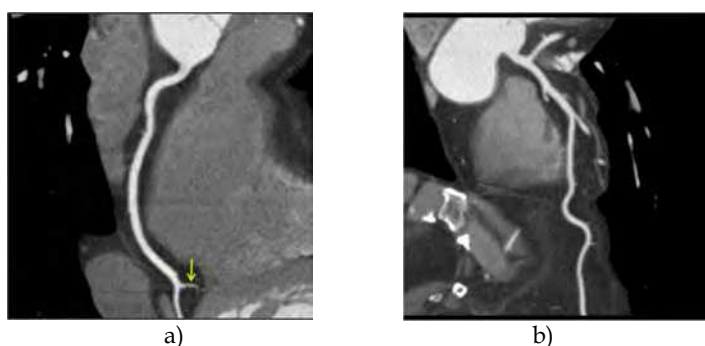a)   b)

Fig. 4. Curved multiplanar reformation of the coronary arteries.

The vessel can be seen in a long length with this technique. Fig. 4a demonstrates a multiplanar reformation of the entire right coronary artery, including a segment of posterolateral marginal branch. The atrio ventricular node artery (arrow) would require a second reconstruction to follow that artery. The left anterior descending (b), with multiple diagonal branches, often needs multiple reconstructions to demonstrate its entire course.

Curved MPR with coronary CT angiography has been reported with high sensitivity and specificity (Achenbach et al., 1998). Significant stenosis and occlusions of the coronary arteries can be visualized with an accuracy that exceeds 90%, since the CT value is preserved, making it fairly easy to delineate calcifications from the lumen. Recognition of calcifications with either higher or lower density than inner lumen contrast is very difficult with VR, somewhat better with MIP, and best with MPR. In addition, curved MPR is used to identify and quantify the degree of stenosis without being hindered by partial averaging (Fig. 5). This method is also useful in delineating the morphology of plaque and its effect on the lumen and adjacent vessel wall. Furthermore, the distance measurements in the curved MPR images represent the true distance. Overall, curved MPR, because they can be rendered quickly and convey all the information about the different CT densities within the vessel, is an extremely useful tool to evaluate contrast-enhanced CT angiography data.

The drawback of curved MPR is that only one vessel can be visualized in one image and that side branches are not depicted unless separate reconstructions are rendered for every side branch (Achenbach et al., 1998). Angiographic view is better in evaluating multiple branches. Furthermore, accurate assessment for stenosis requires correct centerline placement. Since the quality and ability of the computer workstation for tracking the vessel depends on border definition and overall image quality, off-axis centerline placement may happen, which result in misinterpretation of stenosis. Thus, curved MPR requires some editing in most cases. This commonly occurs in the presence of heavy arterial calcification and at the site of origin of branch.

a)

b)   c)   d)
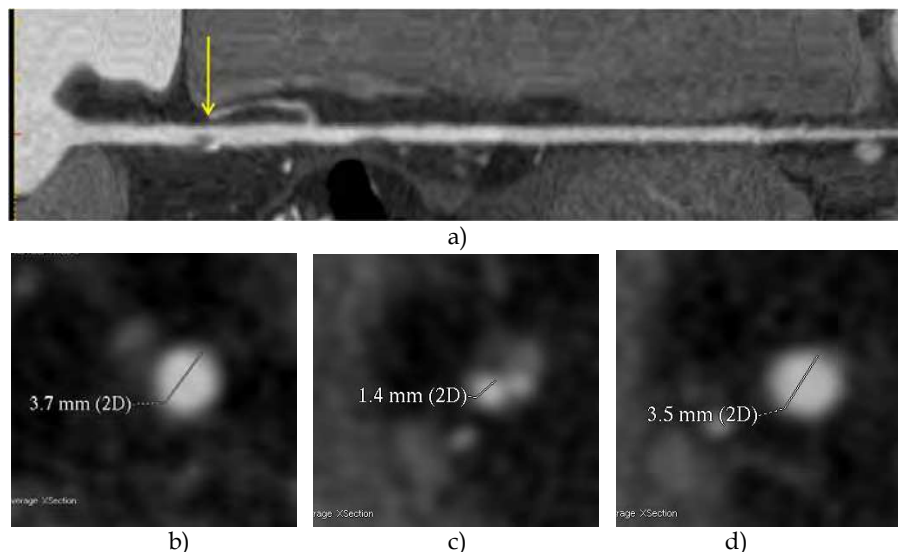
Fig. 5. Curved multiplanar reformation for coronary artery stenosis

Coronary stenosis (arrow) is demonstrated in the proximal segment of the right coronary artery. The observer can always create a plane orthogonal to the direction of the vessel, which allows the evaluation of the configuration of plaque and grading of a stenosis. The three orthogonal planes are at the level of a proximal normal lumen (b), a significant stenosis (c), and a distal normal lumen (d), respectively.

2.4 Volume rendering (VR)

Rendering is a term taken from computer graphics and represents the process of generating a 3D model from a 2D image. Opacity and color are assigned to each CT value interval via transfer function, which is selectable and interactively modifiable (Calhoun et al., 1999). For example, normal soft tissue is assigned high transparency, enhanced vascular structures slight opaqueness and bone strong opaqueness. The sum of all CT values along each search ray from the observer through the 3D data volume, weighted by the transfer function, is displayed. In addition, color is used in most cases, with the color intensity decreasing with increasing distance to the observer in order to generate depth information and a 3D impression. The image can be rotated to different views, allowing the interpreter some flexibility in seeing the segment from multiple angles (Fig. 6).

VR provides an excellent overview of the cardiac and vascular anatomy, such as defining the course of coronary anomalies (Fig. 7a), the presence and course of coronary bypass grafts (Fig. 7b), the analysis of thoracic cardiovascular anatomy and congenital heart disease (Fig. 7c). Because VR creates volumetric 3D representations with the illusion of spatial integrity, it is helpful for surgeons to understand the anatomic complexity before surgery, and for teaching purposes and as illustrations for patients.

It is controversial whether VR can be used for the assessment of coronary stenosis. One study using 16 slice CT compared 3D VRs with combination of techniques including axial images, MPRs, and curved MPRs and MIPs. Sensitivity (63% vs 74%), specificity (80% vs 76%), and accuracy (78% vs 75%) were not significantly different between VR and the combination of techniques, respectively (Cordeiro et al., 2006). However, the diameter of vessels and the apparent thickness of the vessel lumen are dependent on threshold or transparency settings and the computer algorithm that is used to subtract non-vascular structures with VR (Ferencik et al., 2007) (Fig. 8). Furthermore, the overlap of cardiac veins on coronary arteries often hinders the coronary artery stenosis at the overlapped segment on VR (Fig. 9). Another disadvantage of VR is that due to its use of threshold or transparency setting which obscure the lower attenuation structures, the visualization of smaller vessel may be inferior compared with other displaying methods (Johnson et al, 2010). VR also requires several angles to evaluate the entire coronary artery (Fig. 6).

a)   b)

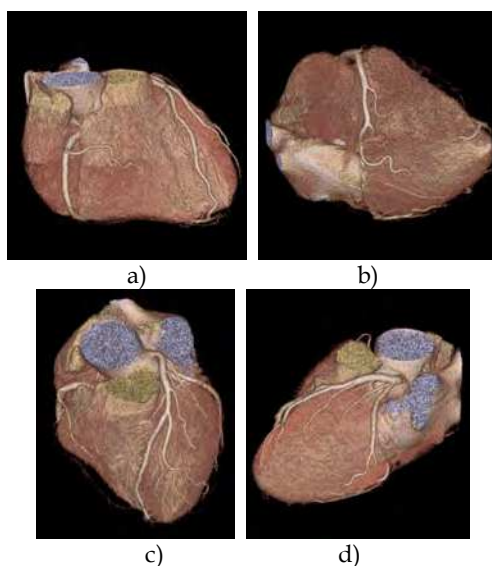c)   d)

Fig. 6. Volume rendering of the coronary arteries.

Volume rendering provides an excellent overview of coronary anomalies, the course of coronary bypass grafts, and congenital heart disease

a. Coronary anomalies: both coronary arteries originate from left coronary cusp (stent is placed in the proximal segment of left descending artery).
b. Bypass grafts: right internal thoracic artery (RITA) graft communicate with the left descending artery and left internal thoracic artery (LITA) graft communicate with obtuse marginal branch.

c. Major aortopulmonary collateral artery in patients with Tetralogy of Fallot (red: aortic arch, yellow: right pulmonary artery arising from aorta, green: left pulmonary arteries arising from ductus arteriosus).

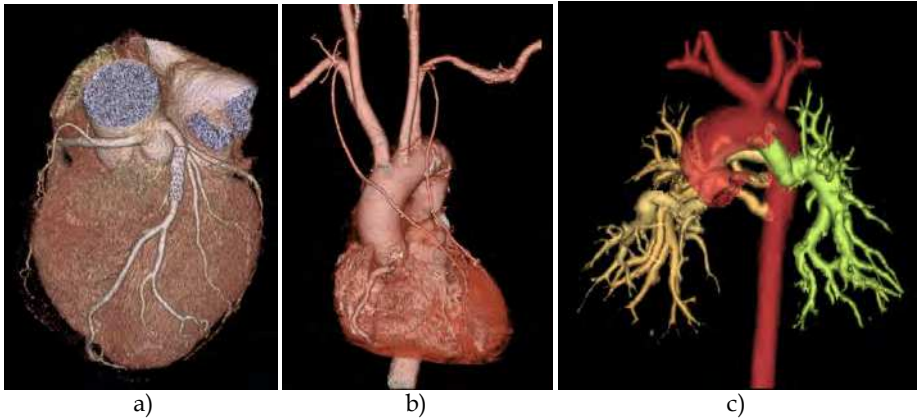a)   b)   c)

Fig. 7. Volume rendering of cardiac and vascular anatomy

Volume rendering allows an easy overview of coronary artery anatomy. It assists significantly in understanding the topography of coronary vessels and position of the lesion in coronary tree. Dedicated projections for each of the three main vessels are performed. The proximal and middle segment of the RCA is visualized in a view from the right side (a). The distal segment of the RCA is visualized in a right caudal view (b). The left anterior descending artery is visualized in a left anterior view (c). The left circumflex artery is visualized in a left cranial view and a left view (d).

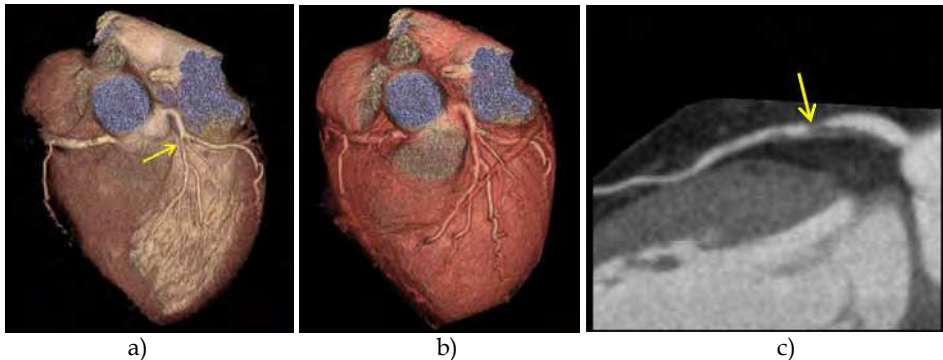a)   b)   c)

Fig. 8. The affect of modifying threshold and opacity setting on volume rendering

Coronary stenosis (arrow) is suspected in the proximal segment of left descending artery in the image with high opacity setting (a), while it is difficult to detect coronary stenosis in the image with low opacity setting (b). Significant coronary stenosis (c: arrow) is seen in curved MPR at the same location suspected in volume rendering with high opacity setting. The diameter of coronary artery is also modified by changing the threshold and opacity setting.
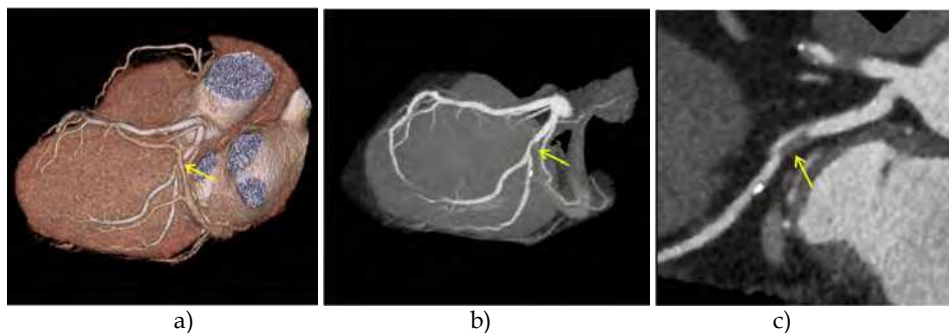
Fig. 9. Overlapped coronary vein on volume rendering

Coronary stenosis in the proximal left circumflex artery (arrow) is hindered by overlapped great cardiac vein on volume rendering (a), while it is well visualized on angiographic view (b: arrow) and curved MPR (c: arrow).

2.5 Angiographic view (AGV)

AGV is an whole heart MIP image in which contrast media of the ventricles is eliminated (Fig.10). This image is similar to that from invasive conventional coronary angiography (CAG). In our institute, AGV images divided into right and left coronary artery were rendered interactively from at least three angles for right coronary artery and six angles for left coronary artery (Fig. 11). If necessary, reconstructions were rendered from additional angles to visualize the entire coronary tree. AGV was originally automatically created only in GE workstation, but is available in many other workstations. It can be created in 3 steps after VR of cardiac CT is created in the usual method (Jinzaki et al., 2006). First, the origins of the right and left coronary arteries are separated from the ascending aorta. Second, the image of the ascending aorta and left ventricle is selected and singled out by clicking any area of the ascending aorta. Third, this image is subtracted from the original cardiac image, which leaves only the image of the coronary artery. Similar images can be created by tracking and extracting the coronary artery itself; however, tracking or extracting requires the threshold of CT attenuation, so the images can vary depending on the threshold and the ability of the workstation being used. AGV keeps the coronary artery untouched, and thus AGV does not vary among workstations.
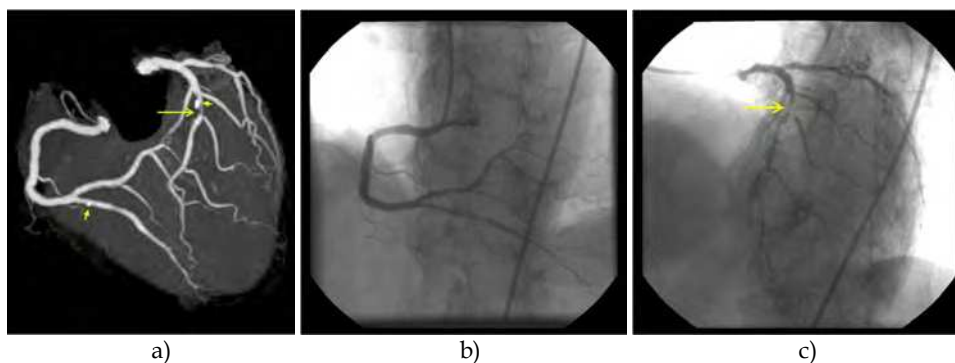

Fig. 10. Angiographic view

Angiographic view image clearly demonstrates the distribution of coronary artery stenosis (long arrow) and coronary calcifications (short arrows) in one image. This resembles the images of coronary angiography and is understandable by third parties. Angiographic view image (a) and coronary angiography (b, c) shows considerable consistency in the detection of coronary artery stenosis (long arrows).
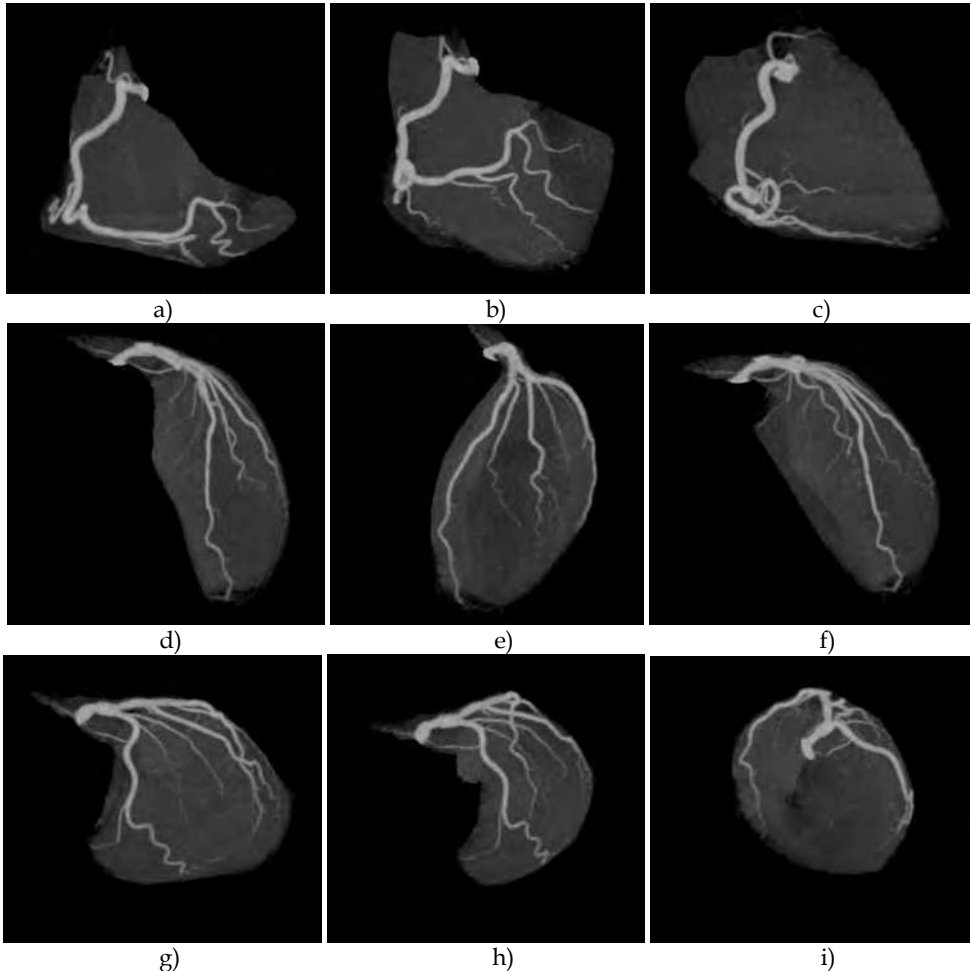

Fig. 11. Angiographic view divided into right and left coronary artery

Angiographic view image divided into right and left coronary artery enables viewing the coronary arteries with the same angle as CAG. We create three directions in RCA [a: left anterior oblique (LAO) 45 and cranial angulations (CRA) 0, b: LAO 20 and CRA 30, c: right anterior oblique (RAO) 30 and CRA 0) and 6 directions in LCA (d: LAO 0 and CRA 30, e: LAO 45 and CRA 25, f: RAO 20 and CRA 40, g: RAO 30 and caudal angulations (CAU) 30, h: RAO 0 and CAU 30, i: LAO 50 and CAU 30].

The advantage of AGV image is that it clearly demonstrates the distribution of high-density lesions, such as coronary calcifications and stents, and coronary artery stenosis in a single image, making it easier to be understood when viewed by any third party. Because the structures are displayed based upon their brightness, calcium and metal are easily distinguished from the contrast-enhanced lumen. For the detection of coronary stenosis, AGV was equally sensitive (98%) and accurate (91%) to a combination of conventional techniques, including interactive MIP and MPR as well as preset curved MPRs (98% sensitive, 94% accurate) (Jinzaki et al., 2009). AGV is also better for displaying small-caliber segments as described in thin-slab MIP. Furthermore, AGV divided into right and left coronary artery enables viewing the lesion with the same angle as CAG, and the detection of best angle of the lesion prior to PCI (Fig. 12). Collateral arteries are also well visualized in AGV. The whole collateral arteries are demonstrated with AGV in less images than volume rendering, since AGV is a projection image (Fig. 13). Thus, AGV would be useful for explaining the severity of disease to the patient, as a guide for the reading due to its high diagnostic accuracy, and in the discussion of the treatment strategy in conference.

Fig. 12. The detection of best angle of the lesion prior to PCI

The coronary stenosis (arrow) is best visualized in the view of RAO 30 and CAU 30 (middle). This information will help cardiologists in discussing treatment strategy and reduce the number of CAG image acquisitions.

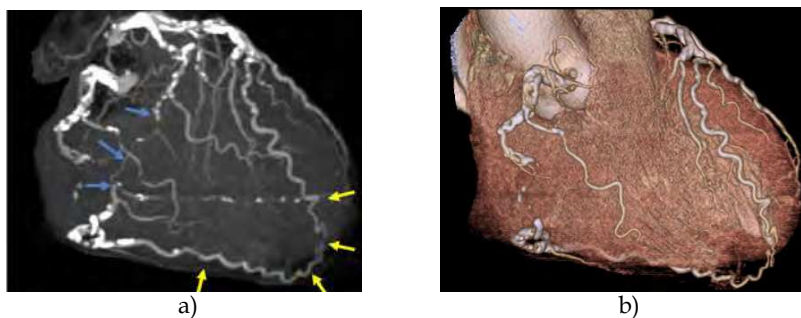a)   b)

Fig. 13. Angiographic view in case with collateral vessels

In patients with chronic total occlusion of RCA, collateral vessels are seen between left descending artery and posterior descending artery (yellow arrows), left circumflex artery and posterolateral artery (blue arrows). These collateral vessels are well demonstrated in one image with angiographic view (a), while the whole collateral arteries are not visualized in one image with volume rendering (b).

A disadvantage of AGV is that since it is a 2D display, it requires review of multiple rotated images to understand 3D relationships. MIP does not provide in-depth information or attenuation detail within the slice, because overlapped higher-density structures obscure the lower-density structures of interest. Static MIP images can be misleading, by incorrect placement of arteries. Another disadvantage is that MIP algorithm is prone to artifacts. One well-known pitfall is the ''string of beads'' appearance, because a normal small vessel passing obliquely through a volume is only partially represented by voxels along its length (Calhoun et al., 1999). Because MIP selects the highest density voxels along a ray projected through the volume, adequate contrast enhancement is imperative. MIP has a tendency to overestimate the stenosis, especially in case with calcification (Rubin et al., 1994). Non-calcified plaque may be overlooked unless it creates significant luminal narrowing, because of its low attenuation value.

2.6 Plaque-loaded angiographic view (PLAG)

So far, there is no post-processing technique that can display an overview image of the lumen and vessel wall of a whole heart in one image (Fig. 14). PLAG is the image in which the non-calcified plaque image is merged with the AGV (Jinzaki et al., 2008). As a result, PLAG allows the noninvasive visualization of the whole coronary lumen and the vessel wall in one image. PLAG is now available in GE workstation and some other workstations. If this is not available in your workstation, it can be generated as follows: First, the color-coded plaque image of each coronary artery is created (Fig 14a). The CT attenuation of the coronary lumen is usually larger than 250HU, while that of non-calcified plaque is typically less than 120HU. Setting the color code range at less than 120 HU can generate a "plaque image", in which only the vessel wall and the non-calcified plaques are color-coded. Second, AGV image of the entire coronary artery (Fig 14b), which is similar to that shown by a CAG is separately generated, which displays the distribution of calcified plaques as well as the lumen in more detail. Third, the color-coded "plaque image" in curved MPR is re-formatted into a MIP image to merge with AGV image. Finally, loading the MIP "plaque image" onto AGV image completes the process (Figs 14c). The critical factors in PLAG are that the merged images are both in MIP format, and taking advantage of a relatively large CT attenuation discrepancy between the lumen and non-calcified plaque allows color-coding, which helps to better visualize plaques when loaded onto AGV.

PLAG will provide comprehensive information for coronary CT angiography in discussing the treatment strategy of both coronary stenosis and non-stenotic non-calcified plaques. This image also enables the overview of the tortuous vessel in the chronic total occlusion (CTO), which would be useful for the percutaneous revascularization of CTO (Fig.15).

In future, with the further improvement of temporal and spatial resolution of MDCT, and with enhanced accuracy of plaque volume quantification is enhanced, this image could also be useful in evaluating and demonstrating the therapeutic effect of anti-atherosclerotic drugs in patients with multiple soft plaques in coronary arteries (the so-called vulnerable patients) on one image.

The characteristics of each post-processing

For the effective use of the various post-processing techniques, knowledge of the characteristics of each post-processing method is mandatory. The strengths and weaknesses of the available post-processing technique are summarized in Table 1.
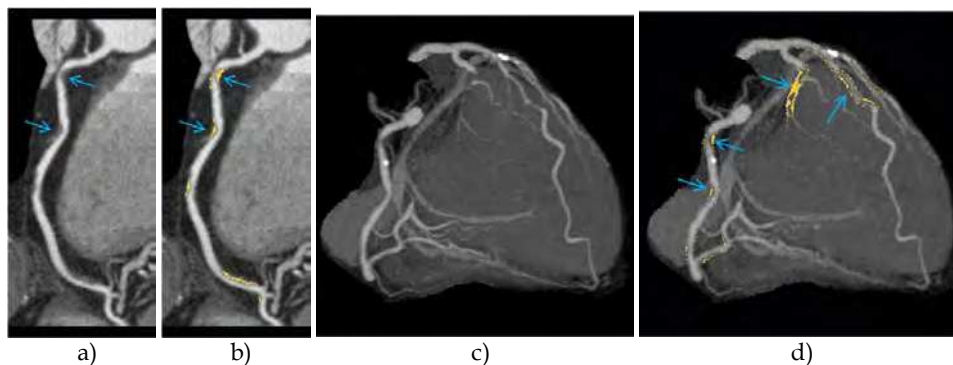
Fig. 14. Plaque-loaded Angiographic View of multiple non-calcified plaques

Curved MPR of the right coronary artery (a) demonstrates the non-stenotic non-calcified plaques (arrows), which are assigned blue in color-coded image (b). The angiographic view image (c) demonstrates the lumen of the entire coronary artery. The color-coded image in curved MPR is re-formatted into a MIP image and merged with the Angiographic View image. The Plaque-loaded Angiographic View image (d) demonstrates the lumen and multiple plaques (arrows) of coronary arteries in one image.
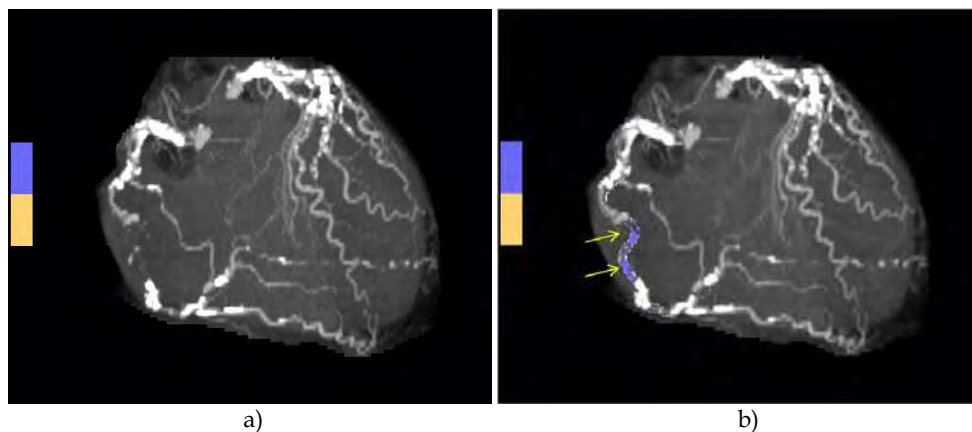

Fig. 15. Plaque-loaded Angiographic View of chronic totally occlusion
An angiographic view image (a) could not provide the information of the occluded lesion. The Plaque-loaded Angiographic View image (b) demonstrates the overview of the tortuous vessel (arrows) in the occluded lesion.

3. Image interpretation

At the beginning of interpretation, an overview of the data set should be performed to detect artifacts, gross abnormalities and the presence of non-coronary cardiac or extra-cardiac abnormalities. Coronary artery interpretation is then performed using post-processing images

Type of technique	Advantage	Disadvantage
Segment evaluation		
Axial image	true data	numerous images required for overview
	anatomical overview	improper for coronary stenosis evaluation
	quick review	
MPR	true data	numerous images required for overview
	anatomical overview	improper for coronary stenosis evaluation
	accurate distance measurements	
	quick review	
Thin-slab MIP	partial overview of the interested vessel	many images required for overview
	high visualization of small vessel	overestimation of coronary stenosis
	quick review	
The entire artery and segment evaluation		
Curved MPR	overview of one entire coronary artery	many images for branch evaluation
	accurate distance measurements	manual editing
	coronary stenosis evaluation	
Whole image		
VR	anatomical overview	user dependent (threshold and transparency setting)
		improper for coronary stenosis evaluation
		low visualization of small vessel
AGV	overview of coronary stenosis	no in-depth information
	high visualization of small vessel	prone to artifact
		low visualization of non-stenotic plaque (non-calcified)
PLAG	overview of stenosis and	no in-depth information
	non-stenotic plaque	prone to artifact
	high visualization of small vessel	Not yet accurate for quantity evaluation of plaque volume

Table 1. Comparison of post-processing techniques

3.1 Examination of image quality

It is imperative that an interpreter spend the first minute making sure the dataset is adequate. Artifacts due to motion, calcification, and metallic densities; image noise; and poor contrast enhancement may degrade the quality of the study as well as simulate or obscure coronary stenoses (Achenbach et al., 2003, Ferencik et al, 2003). To evaluate the image quality, the axial CT source images, multiplanar reformatted images, and also three-dimensional images were analyzed. The reader should specifically state if an artery or artery segment is not interpretable and why.

3.1.1 Artifact

"Artifact" can be defined as any discrepancy between the reconstructed Hounsfield values in the image and the true attenuation coefficients of the object in such a way that these discrepancies are clinically significant or relevant as judged by the radiologist (Hsieh, J., 2003). Artifacts of coronary CT angiography were classified into three categories (Table 2). The first is cardiac motion-related artifact (Choi et al., 2004). This is caused by many factors, including a heart rate greater than 70–75 beats per minute during imaging acquisition, variations in heart rate during breath holding (Fig 16), arrhythmia, and inappropriate selection of pitch or reconstruction window. Artifacts are classified into two patterns: motion blurring or stepladder effects. Blurring occurs when movement in the cardiac structure of interest exceeds the temporal resolution of scanning, either because of a fast heart rate or because of an inappropriate selection of the reconstruction window for the particular coronary artery. Stepladder artifacts are due to motion occurring between reconstruction of sequential heartbeats. The easiest way of reducing cardiac motion artifacts is to lower the heart rate by the prior administration of-blocker. Customized reconstructions at a different cardiac phase may be successful by either adjusting the phase of reconstruction or removing data from undesirable beats.

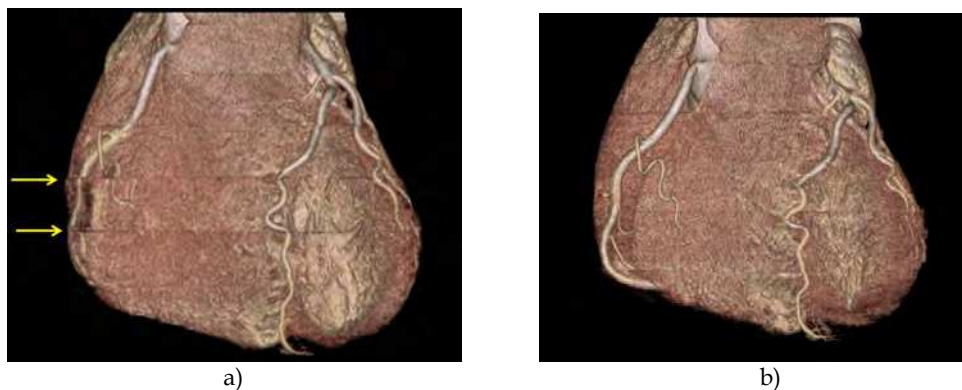a)   b)

Fig. 16. Stepladder artifact due to changing heart rate during CT acquisition. Volume-rendered image (a) shows a severe motion-related artifact (arrows) caused by acceleration in heart rate toward the end of the breath hold. Selection of an optimal reconstruction window reduced the artifact (b).

The second is voluntary motion that is generally preventable with careful instruction of the patient (Choi et al., 2004). Artifacts due to breathing (Fig 17) or body motion are distinctive because they affect the bones of the anterior or lateral chest wall in addition to the coronary arteries; these are less likely to be correctable by additional reconstructions. Oxygen supplementation may help dyspneic patients hold their breaths for a longer period.

The third is high-attenuating artifact (Choi et al., 2004). High-attenuating artifact includes, blooming artifacts, beam hardening artifacts and streaking artifacts. Blooming artifact is a result of partial-volume effects, causing the status that small high-contrast objects appear larger than they are. These artifacts commonly make calcified plaque (Fig 18a) and stents appear to narrow the lumen more than they actually do. Use of appropriate reconstruction filters may reduce these artifacts. Beam hardening presents as dark banding between dense objects. These are also seen in calcified plaque and stents (Fig 18b). Streaking artifact is a kind of reconstruction artifact due to undersampling, photon starvation, motion, beam

hardening, or scatter. In coronary CT angiography, these are usually caused by metallic objects such as clips, markers, and wires used in coronary artery bypass surgery, and often called as metal artifact (Fig 18c).
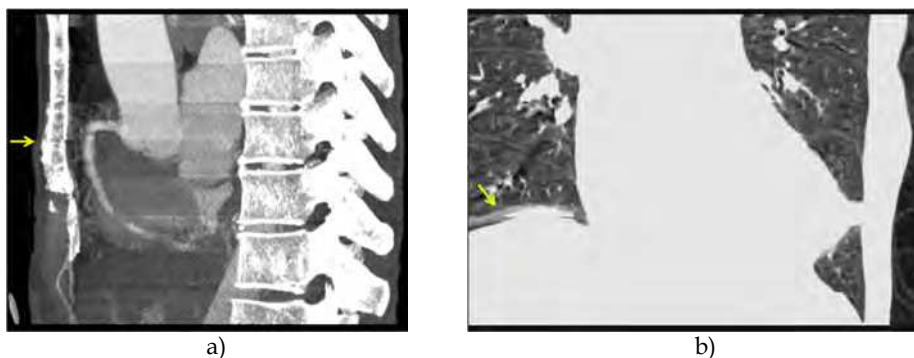

a) b)

Fig. 17. Stepladder artifact due to breathing

Sagittal maximum intensity projection image (a) and coronal MPR image (b) show a severe respiration-related artifact in the anterior chest wall (arrow) and at the diaphragm (arrow).
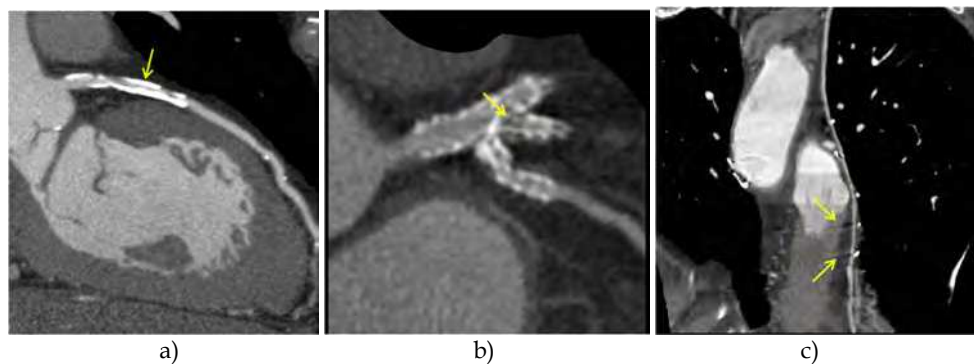

a) b) c)

Fig. 18. High-attenuating artifacts

a. Blooming artifact caused by severe coronary calcifications that interfere with the evaluation of luminal stenosis.
b. Beam hardening artifacts caused by coronary stent that prevents accurate evaluation of the stent lumen.
c. Metal artifacts caused by surgical clips.

3.1.2 Image noise

Improper scan parameter (low tube output for a given body size) causes poor signal-to-noise (Fig 19). This is mainly due to obesity. Improper reconstruction during a part of the cardiac cycle with reduced tube current from EKG-guided tube modulation also results in low image quality.

Fig. 19. Low image quality due to improper scan parameters.

Poor signal-to-noise is caused by low tube output for a given body size

3.1.3 Low contrast enhancement

The methods of reconstruction rely on Hounsfield units (HU) to make images. Values of 250 HU and above are ideal, and current protocols generally yield mean enhancement levels in the range of 300 to 350 HU for right and left coronary arteries (Johnson et al., 2009, Husmann et al., 2009). Low contrast attenuation may be secondary to improper image acquisition timing or slow contrast injection.

Artifact	Cause	Manifestation	Solution
Cardiac motion	High heart rate	Blur	Prior administration of beta-blocker
	Heart rate change	Stepladder artifact	Selection of appropriate reconstruction Window
	Premature contraction	Stepladder artifact	Removing data from undesirable beats
	Inappropriate reconstruction window	Blur	Selection of appropriate reconstruction window
Voluntary motion	Respiration	Blur & stepladder artifact	Oxygen supplementation;
		Careful instruction to patient	
	Body motion	Blur &Stepladder artifact	Minimization of anatomic coverage
			Careful instruction to patient
High-attenuating	Metallic object (Surgical clip, marker, or wire)	Beam hardening Streaking artifact	Use of nonmetallic materials
	Coronary stent	Blooming artifact	Use of appropriate image filters
		Beam hardening	
	Calcification	Blooming artifact	Use of appropriate image filters
		Beam hardening	

Table 2. Various artifacts in coronary CT angiography

3.2 Non-coronary cardiac findings

Non-coronary cardiovascular structures include the pericardium, cardiac chambers, interatrial septum, interventricular septum, atrioventricular valves, ventriculo-arterial valves, pulmonary arteries, pulmonary veins, thoracic aorta, imaged aortic branch arteries, and central systemic veins. The axial images or MPRs is useful for a general understanding of the spatial relationship of these structures and abnormality. Left ventricular and left atrial myocardial walls and chamber cavities should be examined for hypertrophy, dilation, thinning (Fig. 20a), hypodense enhancement, thrombus (Fig 20b), masses, and congenital anomalies. These structures should be reviewed within the cardiac field-of-view and any abnormalities described.
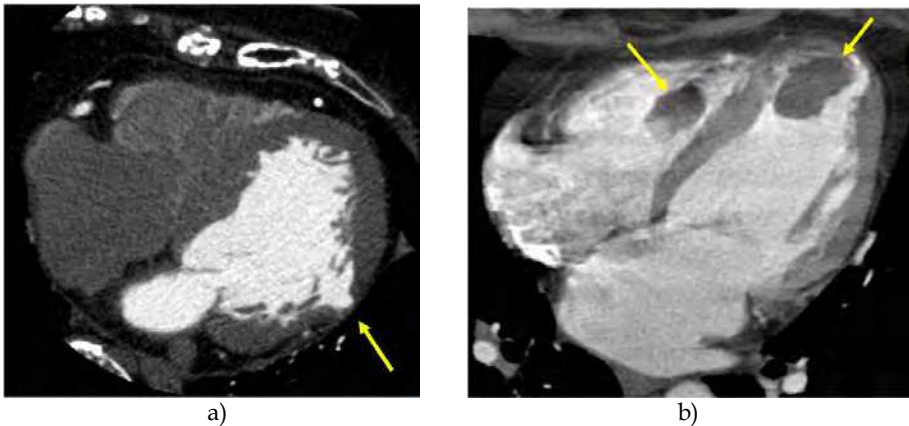

a)   b)

Fig. 20. Non-coronary cardiac findings

a.   Focal thinning of myocardial wall due to ventricular diverticula (arrow)
b.   Thrombus in ventricular chamber (arrow)

3.3 Extra-cardiac structures

Extra-cardiac structures within the field of view of routine coronary CT angiography include the mediastinum, hilum, trachea and bronchi, lung parenchyma, pleura, chest wall, esophagus, stomach, liver, spleen, and colon. Interpretation of the axial images or MPR provides a general understanding of the anatomic relationships of the heart and coronary arteries with surrounding extra-cardiac structures. Review of all visible non-cardiovascular structures is important for two principal reasons: (1) recognition of primary and secondary comorbid pathology and (2) identification of findings that lead to alternative non-cardiovascular diagnoses.

3.4 Coronary artery interpretation

In analyzing coronary arteries, a systematic approach using axial images and post-processing images should be followed. Realizing from the outset that no single method of analysis is without limitations, the incorporative review of the 2D images and the different 3D renderings is necessary. However, how to use the various available post-processing techniques remains a matter of personal experience and may differ among various operators.

3.4.1 Interpretation of axial images

The axial image evaluation is a fundamental and essential step, because information from the original data set (axial images) can be lost as a consequence of processing the images for advanced postprocessing methods. Scrolling through the axial images in the cranio-caudal direction allows interpretation of the anatomy and gross abnormality of coronary arteries. Myocardial bridge of coronary artery is often easily noticed in axial images than post-processing images (Fig 21a). However, following each segment on each level (over 50-80contiguous images) may be difficult, and the evaluation of coronary stenosis is often more difficult compared with the post-processing methods (Jinzaki et al., 2009) (Fig 21b). For example, correct diagnosis of coronary stenosis is difficult with the axial images in the lesions located in the segment running horizontal to the axial section. Diffuse concentric plaque with positive remodeling also has a tendency to be incorrectly viewed as stenotic on axial images, possibly because the reference diameter (vessel diameter in non-diseased artery immediately proximal to the lesion) of these lesions is not measurable on the axial image. The post-processing image is better suited for evaluation of these types of lesions.

a)   b)
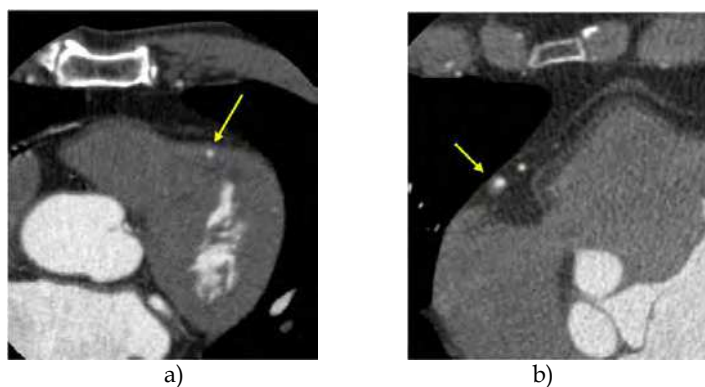
Fig. 21. Interpretation of axial images

Myocardial bridge of coronary artery (a: arrow) is often easily noticed in axial images. The diagnosis of coronary stenosis is easy in the lesions located in the segment running the cranio-caudal direction (b: arrow), however difficult in the lesions located in the segment running horizontal to the axial section.

### 3.4.2 The use of post-processing images

After the interpretation of axial images, the readers should shift to post-processing images. VR provide an overview of the coronary tree. Also, more complex anatomy (such as congenital heart disease or bypass grafts) is easily seen. For coronary artery evaluation, the combination of several types of post-processing algorithms such as thin-slab MIP, MPR and curved MPR is usually used. However, these methods require numerous images to evaluate the whole coronary artery, while AGV would be easy to overview the distribution of coronary lesion. Thus, as an initial guide for the interpretation, we recommend first to use AGV. Furthermore, in the comparison of the AGV image and combination of several types of post-processing, sensitivity was the same (98%) and there was no significant difference in accuracy (Jinzaki et al., 2009). If coronary artery stenosis is detected on AGV, the lesion

should be evaluated further for vessel wall morphology and composition using curved MPR. Further evaluation could be omitted in branch vessels with no stenotic lesions on AGV, since the negative predictive value of AGV is very high (99%) and evaluating multiple diagonal branches or obtuse marginal branches is time-consuming with curved MPR or other methods. However, even if stenotic lesion is not detected in three main arteries on AGV, we recommend reconstructing curved MPR of these arteries to evaluate non-stenotic non-calcified plaque, which may be missed on AGV. This is because acute myocardial infarction is frequently related to a segment that was not significantly stenosed at previous angiography (Littele, et al., 1988, Giroud et al., 1992). Acute coronary occlusions leading to myocardial infarction tend to cluster in predictable "hot spots" within the proximal third of the coronary arteries (Wang et al., 2004). Identification of low attenuation plaques in these high-risk zones for acute coronary occlusions will be important for potentially locally directed preventive strategies.
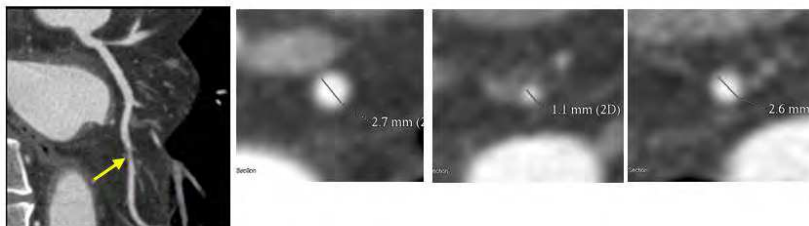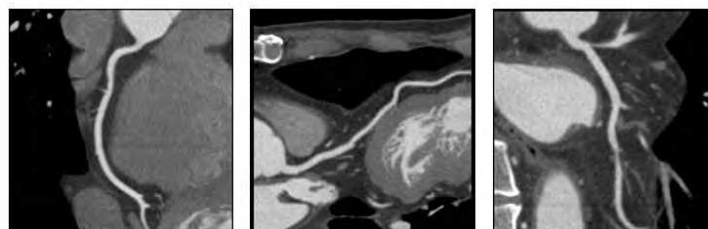

Fig. 22. Workflow of post-processing and interpretation for coronary artery evaluation

Step 1. Overview of coronary artery on angiographic view
Step 2. Quantitative evaluation of coronary lesions detected on angiographic view
Step 3. Evaluation of three main arteries using curved MPR and no further evaluation in branch vessels without stenotic lesions on angiographic view

3.4.3 The guiding principles of interpretation

To analyze coronary arteries a systemic approach should be followed. It is recommended that the coronary segments are evaluated in a sequential order from segment 1 to segment 15 following the standard report of the American Heart Association. The interpretation of coronary arteries include (1) assessment of stenosis severity, (2) vessel wall morphology and composition, (3) total occlusions, and (4) bypass graft and stent.

a. Assessment of stenosis severity

The description of luminal stenosis grading and plaque length is important in the interpretation. The degree of coronary stenosis is manually calculated by subtracting vessel diameter at the site of maximal stenosis from the mean of the vessel reference segment diameters (proximal and distal references) and then dividing the difference by the mean of the vessel reference segment diameters on curved MPR and cross-sectional image (Fig 22). Recent cardiac- vessel analysis packages enables calculating percent stenosis automatically when the user selects the area of maximum narrowing and normal vessel proximal and distal to the stenosis (Busch et al., 2007). However, current spatial resolution of CT has not demonstrated sufficient reproducibility or accuracy in predicting findings of CAG to make such measurements a routine requirement. Thus, at the present time, Society of Cardiovascular Computed Tomography guideline recommends that arterial segments be described within broad stenosis ranges (Cheng et al., 2008, Raff et al., 2009) (Table 3), although future technical developments may improve the precision of stenosis quantification.

0 Normal: Absence of plaque and no luminal stenosis
1 Minimal: Plaque with <25% stenosis
2 Mild: 25%–49% stenosis
3 Moderate: 50%–69% stenosis
4 Severe: 70%–99% stenosis
5 Occluded

Table 3. Quantitative Stenosis Grading

b. Vessel wall morphology and composition

Vessel wall morphology and composition are important information of coronary CT angiography, since these are not available on CAG. coronary CT angiography can visualize intramural presence of positively remodeled plaque and differentiate calcific, non-calcific, and mixed plaque. Society of Cardiovascular Computed Tomography recommends that the description of plaques as ''non-calcific'' is preferable to ''soft'' or ''lipid-rich'' since low CT density (in Hounsfield units) levels do not necessarily correlate closely with anatomic pathology or biochemistry (Raff et al., 2009). Recent studies revealed that the CT characteristics of plaques associated with ACS include positive vascular remodeling, low plaque density<30HU, and spotty calcification (Motoyama et al., 2009) (Fig. 23). Thus, the description of these features will assist interpretation. The

vascular remodeling index is defined as lesion diameter/reference diameter, and is reported as positive when the diameter at the plaque site was at least 10% larger than the reference segment. Spotty calcification was defined when the calcification is <3 mm in size. Features of plaque morphology such as ulceration, dissection, and fissuring are also noted when image quality is sufficient.
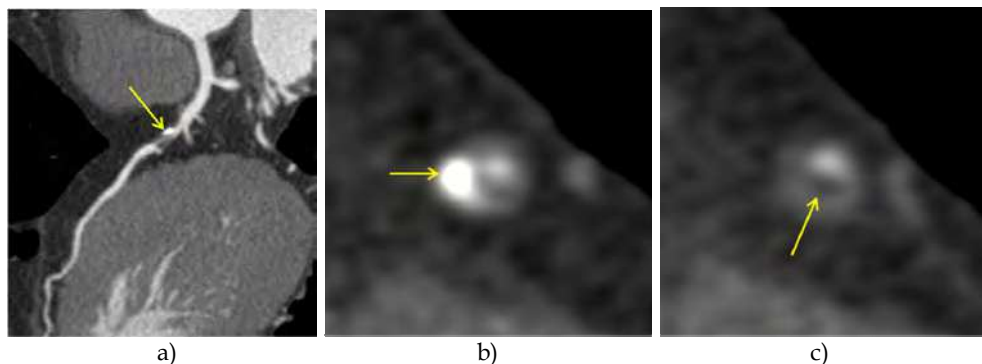

a)   b)   c)

Fig. 23. Low attenuation plaque and spotty calcification

Curved MPR demonstrates significant stenosis in left descending artery (a: arrow). The lesion is accompanied with spotty calcification (b: arrow) and area < 30HU (c: arrow).

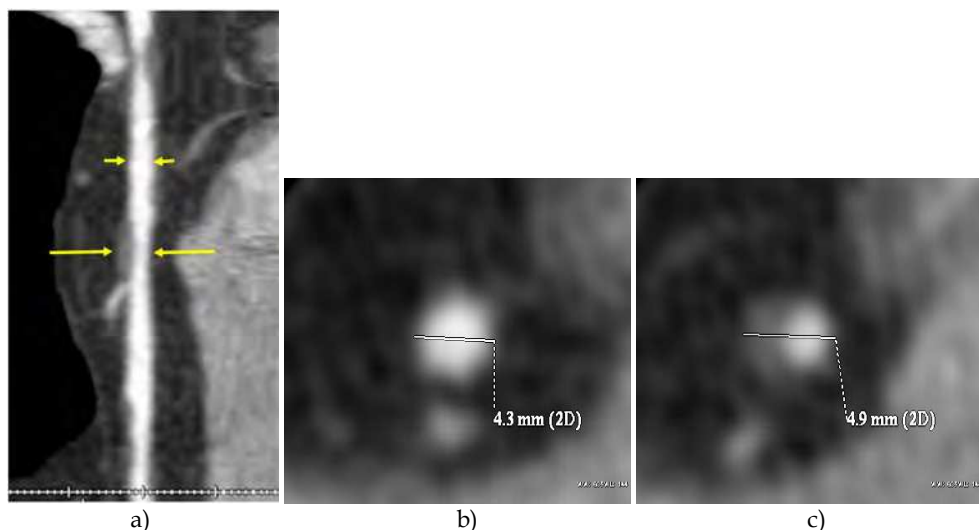a)   b)   c)

Fig. 24. Positive remodeling

Non-calcified plaque (a: long arrows) in right coronary artery is positively remodeled as compared with the normal coronary segment proximal to the lesion (short arrows). The diameter was 4.3 mm in normal segment (b) and 4.9 mm in the lesion (c). Remodeling index was 1.14.

c. Total occlusions

PCI of CTO has a lower success rate than PCI of non-occluded coronary stenosis. Failure of guide-wire crossing the occluded lesion is the main cause of unsuccessful PCI of CTO. Coronary CT angiography may provide useful information for selecting patients suitable for PCI of CTO (Soon et al., 2007). It can show the collateral supply in the distal vessel beyond the occlusion (Fig. 13). The proximal and distal ends of an occluded segment can be distinctively seen on coronary CT angiography. Therefore, the occlusion length can be measured on CCTA (Fig. 24). Mollet et al. also reported that CTO lesion length > 15 mm measured on CT was associated with higher failure rate of PCI (Mollet et al., 2005). Heavy calcification of CTO has been reported to be an independent predictor of failed PCI of CTO (Noguchi et al., 2000). The exact location of calcified plaque on the image of coronary CT angiography may help the interventionist to steer the guide wire away from the calcified lesion that is not well seen on conventional angiography. PLAG images are able to demonstrate the overview of occluded lesion, which are helpful in providing the roadmap for interventionists during the process of wiring the occluded vessel (Fig. 15).

a)   b)
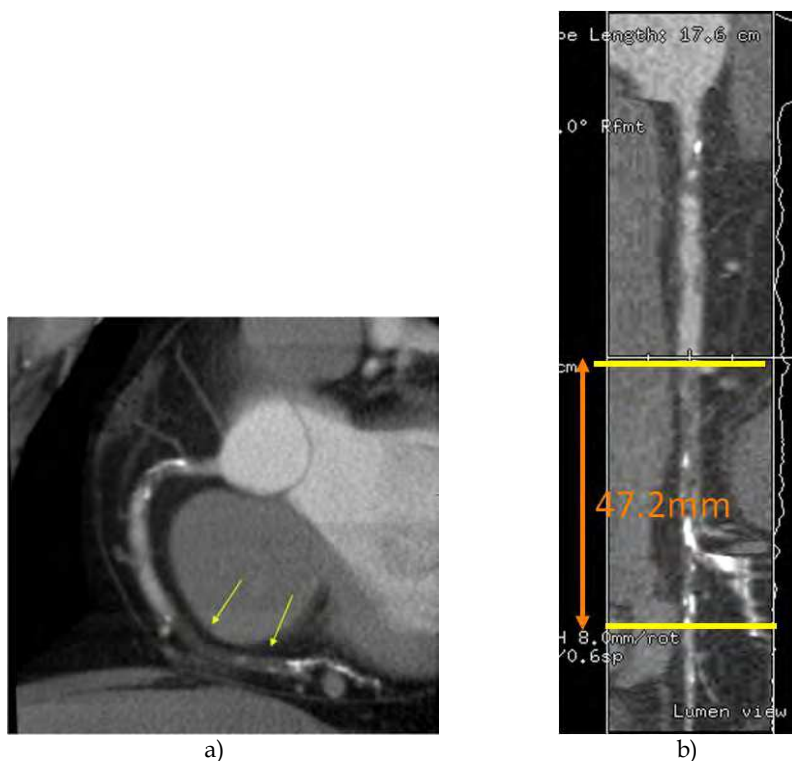
Fig. 25. CT evaluation of chronic total occlusion

The total occlusion is seen in the distal segment of right coronary artery on thin-slab MIP images (a: arrows). The occlusion length can be measured on stretched MPR (b). Calcified plaque is also well visualized.

d. Bypass grafts, stents

The evaluation of coronary bypass grafts by coronary CT angiography is highly accurate in predicting the findings on invasive coronary angiography (Meyer et al., 2007). The location and anastomoses of bypass grafts should be described in addition to the location and severity of stenoses. The evaluation of stents by MDCT is often difficult due to blooming artifact and beam hardening effects. The evaluation of in-stent stenosis depends highly on stent size and composition. Stents 3.0 mm or larger (85%) were judged assessable; 26% of stents smaller than 3 mm were judged assessable (Schroeder et al., 2008). Different stent compositions and structures appeared to be associated with variations in the extent of residual artifact. The use of special reconstruction algorithms improved visualization of the stent lumen and reduced blooming artifact with a drawback of a modest increase in noise in the images (Maintz et al., 2006).

4. Conclusion

Many post-processing images are available for the evaluation of coronary artery. The interpreter should know the advantage and disadvantage of each post-processing image, and perform the incorporative review of the 2D images and the different 3D renderings.

5. References

Achenbach, S., Moshage, W., Ropers, D., & Bachmann, K. (1998). Curved multiplanar reconstructions for the evaluation of contrast-enhanced electron beam CT of the coronary arteries. *AJR Am J Roentgenol,* Vol.170, No.4, (Apr 1998), pp. 895-899.

Achenbach, S., Giesler, T., Ropers, D., Ulzheimer, S., Anders, K., Wenkel, E., Pohle, K., Kachelriess, M., Derlien, H., Kalender, WA., Daniel, WG., Bautz, W., & Baum, U. (2003). Comparison of image quality in contrast-enhanced coronary-artery visualization by electron beam tomography and retrospectively electrocardiogram-gated multislice spiral computed tomography. *Invest Radiol*, Vol.38, No.2, (Feb 2003), pp. 119–128.

Busch, S., Johnson, TR., Nikolaou, K., von Ziegler, F., Knez, A., Reiser, MF., & Becker, CR. (2007). Visual and automatic grading of coronary artery stenoses with 64-slice CT angiography in reference to invasive angiography. *Eur Radiol*, Vol.17, No. 6, (Jun 2007), pp.1445-1451.

Cademartiri, F; Mollet, NR & Nieman, K. (2005). Image post-processing, In *Computed Tomography of the Coronary Arteries*, Feyter PJ & Krestin GP, (ed.), 27-46, Taylor & Francis, New York

Calhoun, PS., Kuszyk, BS., Heath, DG., Carley, JC., & Fishman, EK. (1999). Three-dimensional volume rendering of spiral CT data: theory and method. *Radiographics,* Vol.19, No.3, (May-Jun 1999), pp. 745-764.

Cheng, V., Gutstein, A., Wolak, A., Suzuki, Y., Dey, D., Gransar, H., Thomson, LEJ., Hayes, SW., Friedman, JD., & Berman, DS. (2008). Moving beyond binary grading of coronary arterial stenoses on coronary computed tomographic angiography: insights for the imager and referring clinician. *J Am Coll Cardiol Imaging,* Vol.1, No. 4, (Jul 2008), pp. 460-471.

Choi, HS., Choi, BW., Choe, KO., Cho,i D., Yoo, KJ., Kim, MI., & Kim, J. (2004). Pitfalls, artifacts, and remedies in multi- detector row CT coronary angiography. *Radiographics*, Vol.24, No.3, (May-Jun 2004), pp. 787-800.

Choi, JW., Seo, JB., Do, KH., Choi, SI., Lee, W., Ko, SM., Lee, SH., Lee, JS., Song, JW., Song, KS., & Lim, TH. (2006). Comparison of transaxial source images and 3-plane, thin-slab maximal intensity projection images for the diagnosis of coronary artery stenosis with using ECG-gated cardiac CT. *Korean J Radio,l* Vol.7, No.1, (Jan-Mar 2006), pp. 20-27.

Cordeiro, MA., Lardo, AC., Brito, MS., Rosário Neto, MA., Siqueira, MH., Parga, JR., Avila, LF., Ramires, JA., Lima, JA., & Rochitte, CE. (2006). CT angiography in highly calcified arteries: 2D manual vs. modified automated 3D approach to identify coronary stenoses. *Int J Cardiovasc Imaging*, Vol.22, No.3-4, (Jun-Aug 2006), pp.507-516.

Ferencik, M., Moselewski, F., Ropers, D., Hoffmann, U., Baum, U., Anders, K., Pomerantsev, EV., Abbara, S., Brady, TJ., & Achenbach, S.(2003). Quantitative parameters of image quality in multidetector spiral computed tomographic coronary imaging with submillimeter collimation. *Am J Cardiol*, Vol.92, No.11, (Dec 2003), pp. 1257–1262.

Ferencik, M., Ropers, D., Abbara, S., Cury, RC., Hoffmann, U., Nieman, K., Brady, TJ., Moselewski, F., Daniel, WG., & Achenbach, S. (2007). Diagnostic accuracy of image postprocessing methods for the detection of coronary artery stenoses by using multidetector CT. *Radiology*, Vol.243, No.3, (Jun 2007), pp. 696–702.

Fishman, EK., Ney, DR., Heath, DG., Corl, FM., Horton, KM., & Johnson, PT. (2006). Volume rendering versus maximum intensity projection in CT angiography: what works best, when, and why. *Radiographics*, Vol.26, No.3, (May-Jun 2006), pp. 905-922.

Giroud, D., Li, JM., Urban, P., Meier, B., Rutishauer, W. (1992). Relation of the site of acute myocardial infarction to the most severe coronary arterial stenosis at prior angiography. *Am J Cardiol*, Vol.69, No.8, (Mar 1992), pp. 729-732.

Hsieh, J. (2003). Image artifacts: appearances, causes, and corrections. In *Computed tomography: principles, design, artifacts, and recent advance*, Hsieh, J, (Ed.), 167–240, SPIE Press, Bellingham, USA

Husmann, L., Gaemperl,i O., Valenta, I., Schepis, T., Scheffel, H., Stolzmann, P., Leschka, S., Desbiolles, L., Marincek, B., Alkadhi, H., & Kaufmann, PA. (2009). Impact of vessel attenuation on quantitative coronary angiography with 64-slice CT. *Br J Radil*, Vol.82, No.980, (Aug 2009), pp. 649-653.

Jinzaki, M., Sato, K., Tanami, Y., Yamada, M., Kuribayashi, S., Anzai, T., Asakura, Y., & Ogawa, S. (2006). Novel method of displaying coronary CT angiography -Angiographic view-. *Circ J*, Vol.70, No.12, (Dec 2006), pp. 1661-662.

Jinzaki, M., Sato, K., Tanami, Y., Yamada, M., Anzai, T., Kawamura, A., Ueno, K., & Kuribayashi, S. (2009). Diagnostic accuracy of angiographic view image for the detection of coronary artery stenoses by 64-detector row CT: a pilot study comparison with conventional post-processing methods and axial images alone. *Circ J*, Vol.73, No.4, (Apr 2009), pp. 691-698.

Jinzaki, M., Yamada, M., Sato, K., Tanami, Y., Anzai, T., Sasaki, K., & Kuribayashi, S. (2008). Overview Image of the Lumen and Vessel Wall in Coronary CT

Angiography -The Plaque-Loaded Angiographic View-. *Circ J*, Vol.72, No.4, (Apr 2008), pp. 671-673.

Johnson, PT., Pannu, HK., & Fishman, EK. (2009). IV contrast infusion for coronary artery CT angiography: literature review and results of a nationwide survey. *AJR Am J Roentgenol* Vol.192, No.5, (May 2009), pp.W214–221.

Johnson, PT., & Fishman, EK. (2010). Postprocessing techniques for cardiac computed tomographic angiography. *Radiol Clin North Am*, Vol.48, No.4, (Jul 2010), pp. 687-700.

Little, WC., Constantinescu, M., Applegate, RJ., Kutcher, MA., Burrows, MT., Kahl, FR., Santamore, WP. (1988). Can coronary angiography predict the site of a subsequent myocardial infarction in patients with mild-to-moderate coronary artery disease? *Circulation*, Vol.78, No.5, (Nov 1988), pp. 1157-1166.

Maintz, D., Seifarth, H., Raupach, R., Flohr, T., Rink, M., Sommer, T., Ozgün, M., Heindel, W., & Fischbach, R.(2006). 64-slice multidetector coronary CT angiography: in vitro evaluation of 68 different stents. *Eur Radiol*, Vol.16, No. 4, (Apr 2006), pp. 818-826.

Meyer, TS., Martinoff, S., Hadamitzky, M., Will, A., Kastrati, A., Schomig, A., & Hausleiter, J. (2007). Improved noninvasive assessment of coronary artery bypass grafts with 64-slice computed tomographic angiography in an unselected patient population. *J Am Coll Cardiol*, Vol.49, No. 9, (Mar 2007), pp. 946-950.

Mollet, NR., Hoye, A., Lemos, PA., Cademartiri, F., Sianos, G., McFadden, EP., Krestin, GP., Serruys, PW., & de Feyter, PJ.(2005). Value of preprocedure multislice computed tomographic coronary angiography to predict the outcome of percutaneous recanalization of chronic total occlusions. *Am J Cardiol*, Vol.95, No. 2, (Jan 2005), pp. 240–243.

Motoyama, S., Sarai, M., Harigaya, H., Anno, H., Inoue, K., Hara, T., Naruse, H., Ishii, J., Hishida, H., Wong, ND., Virmani, R., Kondo, T., Ozaki, Y., & Narula, J. (2009). Computed tomographic angiography characteristics of atherosclerotic plaques subsequently resulting in acute coronary syndrome. *J Am Coll Cardiol*, Vol.54, No. 1, (Jun 2009), pp. 49-57.

Noguchi, T., Miyazaki, MD S., Morii, I., Daikoku, S., Goto, Y., & Nonogi, H. (2000). Percutaneous transluminal coronary angioplasty of chronic total occlusions. Determinants of primary success and long-term clinical outcome, *Catheter Cardiovasc Interv* Vol.49, No. 3, (Mar 2000), pp. 258–264.

Raff, GL., Abidov, A., Achenbach, S., Berman, DS., Boxt, LM., Budoff, MJ., Cheng, V., DeFrance, T., Hellinger, JC., Karlsberg, RP., & Society of Cardiovascular Computed Tomography. (2006). SCCT guidelines for the interpretation and reporting of coronary computed tomographic angiography. *J Cardiovasc Comput Tomogr*, Vol.3, No. 2, (Mar-Apr 2006), pp.122-136.

Rubin, GD., Dake, MD., Napel, S., Jeffrey, RB Jr., McDonnell, CH., Sommer, FG., Wexler, L., & Williams, DM. (1994). Spiral CT of renal artery stenosis: Comparison of three-dimensional rendering techniques. *Radiology*, Vol.190, No.1, (Jan 1994), pp. 181–189.

Schroeder, S., Achenbach, S., Bengel, F., Burgstahler, C., Cademartiri, F., de Feyter, P., George, R., Kaufmann, P., Kopp, AF., Knuuti, J., Ropers, D., Schuijf, J., Tops, LF., & Bax, JJ.; Working Group Nuclear Cardiology and Cardiac CT; European

Society of Cardiology; European Council of Nuclear Cardiology. (2008). Cardiac computed tomography: indications, applications, limitations, and training requirements: report of a Writing Group deployed by the Working Group Nuclear Cardiology and Cardiac CT of the European Society of Cardiology and the European Council of Nuclear Cardiology. *Eur Heart J,* Vol.29, No. 4, (Feb 2008), pp. 531-556.

Soon, KH., Selvanayagam, JB., Cox, N., Kelly, AM., Bell, KW., & Lim, YL. (2007). Percutaneous revascularization of chronic total occlusions: review of the role of invasive and non-invasive imaging modalities. *Int J Cardiol,* Vol.116, No. 1, (Mar 2007), pp. 1-6.

Wang, JC., Normand, SL., Mauri, L., & Kuntz, RE. (2004). Coronary artery spatial distribution of acute myocardial infarction occlusions. *Circulation*, Vol.110, No.3, (Jul 2004), pp. 278-284.

Zhang, ZH., Jin, ZY., Li, DJ., Lin, SB., Zhang, SY., Kong, LY., Wang, Y., Wang, LH., Zhao, WM., Mou, WB., Zhang, LR., Zhu, WL., Ni, C., Ren, H., Yu, HQ., Miao, Q., & Fang, Q. (2004). Non-invasive imaging of coronary artery with 16-slice spiral computed tomography. *Chin Med Sci J*, Vol.19, No.3, (Sep 2004), pp. 174-179.
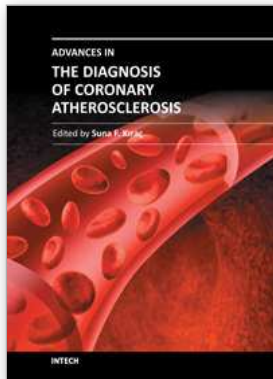
Advances in the Diagnosis of Coronary Atherosclerosis

Edited by Prof. Suna Kirac

Coronary artery disease (CAD) and its consequences are most important morbidity and mortality reasons in the developed and developing countries. To prevent hard end-points, early definitive diagnosis and optimum therapy play significant role. Novel advanced diagnostic tests which are biomarkers of inflammation, cell adhesion, cell activation and imaging techniques provide to get the best result in the detection and characterization of calcified or uncalcified atherosclerotic plaques. In spite of last developments in the imaging methods, coronary catheterization is still frequently performed. Following the first cardiac catheterization performed in 1844, date by date historical developments and the mechanics of cardiac catheterization techniques, risks associated with coronary angiography, and also, preventions and treatments of possible complications have been presented in this book. Other important issue is radiation exposure of patients and staff during coronary angiography and scintigraphy. Radiation dose reduction techniques, general radiation protection principles have been discussed in related chapters.

How to reference

In order to correctly reference this scholarly work, feel free to copy and paste the following:

INTECH
open science | open minds